Secondary Structure of Histones and DNA in Chromatin

Abstract. *Laser Raman spectroscopy indicates that the inner histones which are bound to DNA in chromatin or in isolated nu bodies are similar in conformation to the inner histones which are dissociated from DNA in high-salt solutions. This structure contains, on the average, 51 ± 5 percent α-helix and no substantial β-sheet conformation. It is proposed that the protein core of the nu body has a high α-helix content.*

The nucleohistone component of eukaryotic chromatin is organized as a string of closely packed subunits, called nu bodies or nucleosomes. Each nu body consists of about 140 nucleotide base pairs (bp) of DNA enveloping a protein core which is made up of two molecules each of histones H4, H3, H2A, and H2B (the "inner histones"). Adjacent nu bodies are connected by a nuclease-sensitive stretch of DNA (30 to 70 bp), to which are bound the lysine-rich histones H1 or H5 (*1*).

Large quantities of monomeric nu bodies (ν_1) have recently been prepared, subfractionated, and characterized by various physical methods (*2*). Here we report the laser Raman spectra of these ν_1 preparations and of chromatin, and identify the conformational structures of the constituent DNA and histone molecules.

Laser Raman spectroscopy is a valuable tool for determining the secondary structures of nucleic acids and proteins in aqueous solutions (*3, 4*). Recent applications to viruses and DNA-polylysine complexes demonstrate the utility of the method for investigating nucleoprotein assembly (*5*). The method depends on the ability to obtain, by laser light scattering, a vibrational spectrum consisting of a series of lines (or frequencies) characteristic of the structure or environment of macromolecular subgroups (*3*). The ways in which the Raman frequencies and intensities are used to detect and quantify nucleic acid and protein conformations have been fully discussed (*3–7*).

In the work reported here, samples were contained in sealed capillaries (Kimax No. 34507) of 1.0-mm inner diameter and were thermostated to ± 0.5°C with a device described previously (*8*). Raman spectra were excited with the 488.0-nm line of an argon-ion laser (Coherent model CR2) and recorded on a Spex Ramalog spectrometer. Further details of instrumentation are given elsewhere (*3*).

Raman spectra of H_2O solutions of chicken DNA, the inner histone "heterotypic" tetramer (*9*), chicken erythrocyte ν_1 (*10*), and chicken erythrocyte chromatin are presented in Fig. 1. The DNA and inner histone tetramer were examined in 2*M* NaCl, ν_1 in both 0.2 m*M* EDTA and 2*M* NaCl, and chromatin in 0.2 m*M* EDTA.

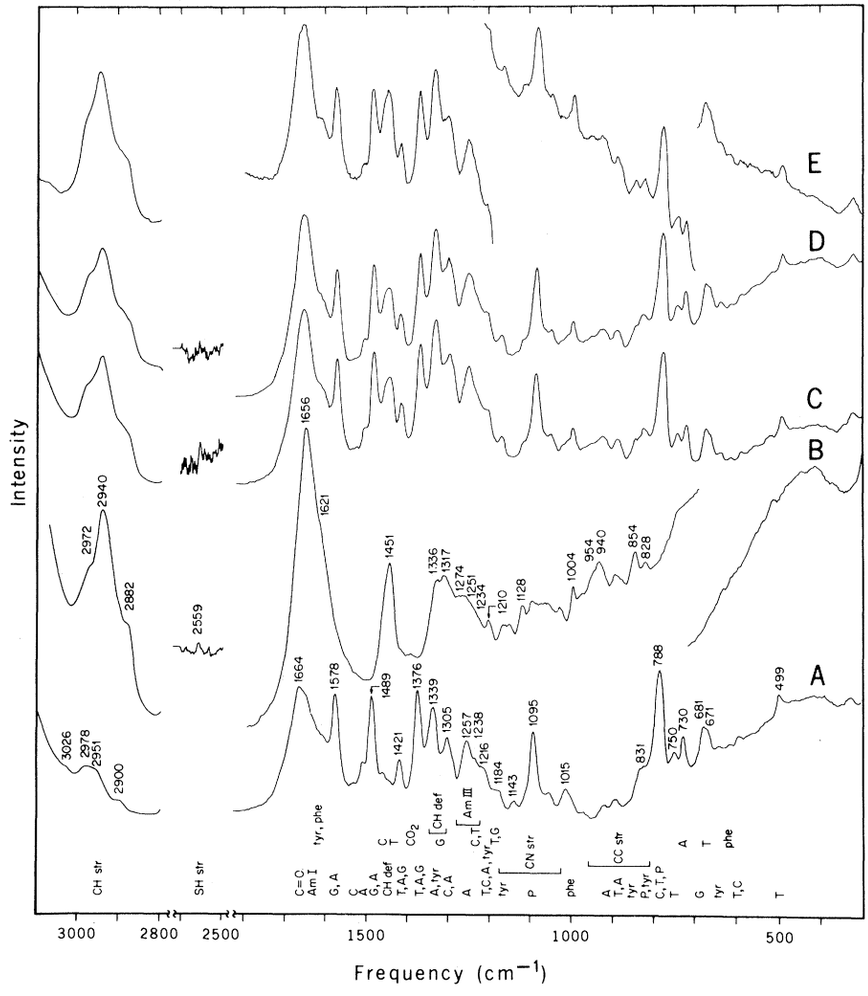

Fig. 1. Raman spectra at 32°C of (A) chicken DNA (4 percent by weight) in 2.0*M* NaCl; (B) inner histones (9 percent) in 2.0*M* NaCl, 10 m*M* tris (*p*H 7), and 0.1 m*M* dithiothreitol (DTT); (C) ν_1 (10 percent) in 0.2 m*M* EDTA; (D) ν_1 (10 percent) in 2.0*M* NaCl and 0.2 m*M* EDTA; and (E) chicken erythrocyte chromatin (26 percent) in 0.2 m*M* EDTA. Conditions: excitation wavelength, 488.0 nm; spectral slit width, 10 cm^{-1}; radiant power, 300 mw; amplification, A = 1 (300 to 1800 cm^{-1}), A = 3 (2500 to 2600 cm^{-1}), and A = 1/3 (2800 to 3100 cm^{-1}). Abbreviations: *str*, stretching; *def*, deformation; *A*, *T*, *C*, and *G*, adenine, thymine, cytosine, and guanine; *P*, phosphate; *phe*, phenylalanine; *tyr*, tyrosine; and *Am*, amide. Chicken DNA was obtained from Sigma Chemical Company. Inner histone heterotypic tetramer was prepared according to published procedures (*9*). The histone extract (0.5 ml of a solution containing 10 mg of protein per milliliter) of chicken chromatin [2.0*M* NaCl, 10 m*M* tris (*p*H 7), and 0.1 m*M* DTT] was layered onto a 5 to 20 percent linear sucrose gradient [2.0*M* NaCl, 0.2 m*M* EDTA (*p*H 7.1), and 0.1 m*M* DTT] and centrifuged in a SW 50.1 rotor, for 48 hours at 48,000 rev/min and 5°C. The tetramer peak was pooled, dialyzed against 2.0*M* NaCl, 10 m*M* tris (*p*H 7), and 0.1 m*M* DTT, and concentrated by negative pressure ultrafiltration in a collodion bag. The fraction of ν_1 soluble in 0.1*M* KCl was concentrated in a collodion bag (*2*) before shipment. Chicken erythrocyte chromatin was prepared by a short-term digestion of isolated nuclei with micrococcal nuclease under conditions employed previously (*2*), except that digestion proceeded for 15 minutes rather than for 6 hours. The digested nuclear pellet was dispersed in 0.2 m*M* EDTA (*p*H 7), dialyzed extensively against 0.2 m*M* EDTA, and centrifuged in a type 65 rotor for 16½ hours at 58,000 rev/min and 5°C before shipment. All samples were prepared at Oak Ridge and were shipped to Southeastern Massachusetts University packed in Dry Ice.

The Raman spectrum of chicken DNA (curve A in Fig. 1) is similar to that of calf thymus DNA (*11*), in accord with base composition data. Spectra of ν_1 (curves C and D in Fig. 1), and to a lesser extent those of chromatin (curve E in Fig. 1), are dominated by Raman scattering of the constituent DNA, which is consistent with the known protein/DNA weight ratios (*2*). In determining DNA secondary structures from these data, we note the occurrence of the PO_2^- group frequency (dioxy symmetric stretching) at 1094 cm^{-1} and the backbone group frequency (predominantly diester –O–P–O– stretching) at 832 cm^{-1} for each sample. This indicates that, in each case, the DNA backbone is in the B-genus conformation (*3, 12*). The relative intensities of Raman lines at 671 and 681 cm^{-1}, due respectively to vibrations of thymine and guanine rings, also indicate the type of base interactions found in double-stranded DNA of the B-genus structure (*13*). The absence of a Raman line near 812 cm^{-1} in DNA, ν_1, and chromatin confirms the absence of A-helical DNA in these samples (*5, 13*).

The purified inner histone tetramer in 2*M* NaCl (curve B in Fig. 1) exhibits clearly distinguishable Raman lines due to amide I (1656 cm^{-1}), CH deformations (1451 cm^{-1}), amide III (broad and weak with components near 1274, 1252, and 1234 cm^{-1}), and aromatic side chains (1004, 854, and 828 cm^{-1}). A very weak line, tentatively assigned to SH stretching, occurs at 2559 cm^{-1}. Other lines assignable to protein subgroups are as noted for curve B in Fig. 1.

The positions and relative intensities of amide I and amide III Raman lines of the inner histones indicate that the protein chain conformations are predominantly α-helical, with substantial amounts of irregular or "random chain" structure. The absence of an intense amide III component below 1240 cm^{-1} makes it unlikely that any appreciable amount of β-sheet structure is present (*4, 14*). The same conclusions are indicated by data from D_2O solutions of inner histones, where Raman lines due to amide I′ and amide III′ vibrations are located at about 1650 and 950 cm^{-1}, respectively (*4*).

To quantify these results we applied a recently described method for computing the percentages of α, β, and random structures from the observed amide I′ and amide III′ Raman lines (*15*). This method yields the following results for inner histones in 2*M* NaCl: 51 ± 5 percent α helix, 36 ± 4 percent random chain, and 13 ± 9 percent β sheet. The limits of error correspond to uncertainties in the measured Raman line intensities and do not include uncertainties inherent in the method of Lippert *et al.* (*15*).

Circular dichroic spectra were also obtained for the purified inner histone tetramer in 2*M* NaCl (Fig. 2A). Percentages of α, β, and random structures were evaluated by the "total spectra" method of Baker and Isenberg (*16*). The required base spectra were those reported for five globular proteins by Chen *et al.* (*17*), and the wavelength range spanned was 207 to 243 nm. The calculation yielded the following results: 50 percent α helix, 51 percent random chain, and 5 percent β sheet. In this method (*16*) the sum of the percentages provides a sensitive and unique test for the adequacy of the reference spectra and, hence, confidence in the accuracy of the results. Our sum of 106 percent compares well with the "best" calculations of Baker and Isenberg (*16*).

Other details of structure which may be inferred from the Raman data for the inner histones are as follows. (i) A single cysteine residue in each inner histone tetramer (that is, one cysteine group for 491 amino acid groups) is revealed by its Raman line at 2559 cm^{-1}. The especially low frequency of the cysteinyl SH stretch [compare with the data in (*5*) and (*6*)] further suggests the possibility of a strong interaction involving the SH group. (ii) There are nine tyrosine residues distributed among the four molecules (or 491 amino acids) of inner histones (*1*). These produce relatively intense Raman lines at 854 and 828 cm^{-1}—the so-called tyrosine doublet. The relative intensities of the two Raman lines of the doublet have been correlated with the state of hydrogen bonding of the parahydroxyl group of tyrosine (*18*). Using this correlation, we conclude that each of the 15 tyrosine residues is involved in a specific hydrogen-bonding interaction, in which the tyrosyl OH group is the acceptor of a strong hydrogen bond from a positive donor group. The most obvious candidates for such hydrogen-bonding interactions are the $-NH_3^+$ terminal groups of lysyl side chains.

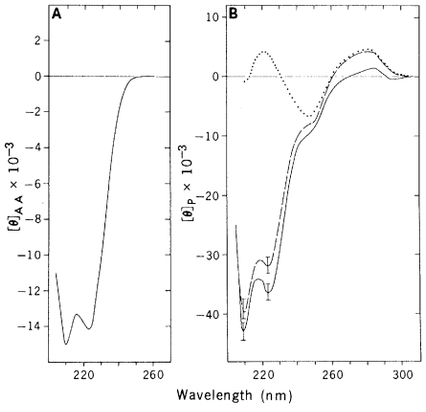

Fig. 2. (A) Circular dichroic spectrum at 25°C of inner histone tetramer in 2.0*M* NaCl, 10 m*M* tris (*p*H 7), and 0.1 m*M* DTT. The total concentration of amino acid residues was estimated by quantitative amino acid analysis of an HCl hydrolyzate. Data are expressed as molecular ellipticity per mole of amino acid residues, $[\theta]_{AA}$. (B) Circular dichroic spectra at 25°C of ν_1 in 0.2 m*M* EDTA (——) and in 2.0*M* NaCl, 10 m*M* tris (*p*H 7), and 0.1 m*M* DTT (-----) compared to the spectrum of chicken DNA (·····) in the same 2.0*M* NaCl buffer. Data are expressed as molecular ellipticity per mole of DNA phosphate, $[\theta]_P$, assuming the absorptivity per mole of DNA phosphate ($\epsilon_{P,260}$) equal to 6500 for DNA and for ν_1. Similar circular dichroic spectra were obtained for ν_1 at the KCl concentrations given in the text. At 0.1*M* KCl, the turbidity of ν_1 precluded obtaining reliable data; at other KCl concentrations a constant $[\theta]_P$ ± 10 percent was observed at 223 nm, with no systematic correlation with the molarity of KCl. The increase in $[\theta]_P$ (260 to 290 nm) of ν_1 due to the dissociation of histones and DNA at high ionic strength has been frequently observed for chromatin (*1*) and may well represent conformational changes of DNA between different states of the B genus of double helices.

Raman spectra were also obtained for inner histones in 2*M* NaCl over the temperature range 0° to 51°C. The spectrum is unchanged from 0° to 50°C, but above 50°C it changes significantly as the protein precipitates from solution. Shifts of amide I to a higher frequency (1662 cm^{-1}) and amide III to a lower frequency (1240 to 1245 cm^{-1}) indicate a loss of α-helical structure with increasing temperature. Similar changes also occur in the Raman spectrum of α-helical poly-L-lysine and are interpreted as indicating replacement of α-helical structure by β-sheet or random structure as temperature increases (*19*).

The Raman spectrum of ν_1 in 0.2 m*M* EDTA (curve C in Fig. 1) reveals several lines assignable to the inner histones: SH stretching of cysteine (2556 cm^{-1}), amide I (1657 cm^{-1}), CH deformations (1451 cm^{-1}), and various modes of amino acid side groups (for example, lines at 1126, 1004, and 851 cm^{-1}). Weaker lines of the protein are also recognizable in the regions 850 to 1000 and 1200 to 1350 cm^{-1}, although specific assignments cannot be made. Since the amide I and amide III modes of ν_1 are similar to those of the inner histones, the protein chain conformations of ν_1 are similar to those of the free inner histones. The facts that the SH stretching line of cysteine is observed in ν_1 and that no strong line attributable to SS stretching appears near 500 to 550 cm^{-1} suggest that no S–S bridge is formed on dimerization of the histone

tetramer to form an octamer in association with DNA. This finding is consistent with other data from our laboratory which show that the cysteinyl SH of ν_1 is "buried" in terms of its reactivity with *N*-ethylmaleimide (NEM). The SH group in question exhibits stoichiometric reactivity (that is, about two NEM's per ν_1) in 10*M* urea or in 1.5 to 2.0*M* KCl (*20*). Although partially obscured by overlapping Raman lines of DNA, the tyrosine doublet is also detectable in ν_1 by virtue of its higher-intensity component (~ 851 cm^{-1}). Moreover, the intensity of the 851 cm^{-1} component of the doublet appears to be the same in ν_1 as in the inner histones, and therefore the hydrogen-bonding interactions mentioned above are probably maintained on association of the inner histones with DNA. It is interesting to note that a similar conclusion applies to the tyrosyl OH groups of α-helical coat proteins of the DNA bacteriophages Pf1 and fd (*7*).

Numerous studies of chromatin and of nu bodies (*1, 9, 21*) indicate that the histones and DNA are completely dissociated from one another in 2*M* NaCl (or KCl) solution. However, there are no significant differences between Raman spectra of ν_1 in 2*M* NaCl (curve D in Fig. 1) and spectra of the same ν_1 in 0.2 m*M* EDTA. As examined by laser Raman spectroscopy, therefore, the secondary conformations of the histone and DNA remain largely unchanged when ν_1 is dissociated by high NaCl concentrations. This is demonstrated more clearly in Fig. 3, where the Raman spectra of ν_1 in 0.2 m*M* EDTA and in 2*M* NaCl are observed to differ little from the sum of spectra of DNA and inner histones (*22*). If the 7-N position of the guanine residue in DNA is involved in DNA-histone interactions, as has been proposed for DNA-polyarginine complexes (*12*), such interactions are not apparent from the present data.

Raman spectra of total, unfractionated ν_1 (*10*) were obtained in 0.2 m*M* EDTA containing KCl concentrations of 0.15, 0.5, 1.0, 2.0, 3.0, 4.0, and 4.6*M*. Since amide I and amide III Raman lines are unchanged over this range of KCl concentrations, the protein conformations of total ν_1 are also apparently unaffected by dissociation. We have employed the ratio of the intensity of Raman scattering at 1451 cm^{-1} (C–H deformation modes of aliphatic amino acids) to that at 1489 cm^{-1} (adenine and guanine ring modes) as a measure of the protein/DNA ratio in different samples. We find that the intensity ratio I_{1451}/I_{1489} of total ν_1 does not change significantly over the range 0.15 to 4.0*M* KCl, even though dissociation of ν_1 is expected to take place within this range (*1, 9, 21*). Only when the histone precipitates from solution (for example, at 4.6*M* KCl) does I_{1451}/I_{1489} drop sharply.

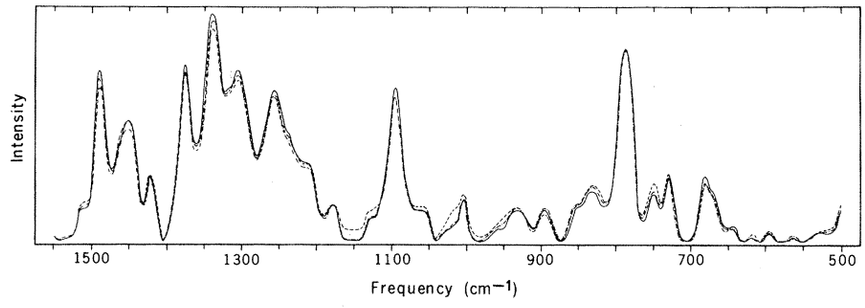

Fig. 3. Comparison of Raman spectra of ν_1 in 0.2 m*M* EDTA containing no added salt (—·—) and in 2.0*M* NaCl (—) with the sum of spectra of the constituent DNA and inner histones (----).

Circular dichroic spectra of ν_1 were also obtained in 0.2 m*M* EDTA, or in 0.2 m*M* EDTA containing 0.1, 0.3, 0.5, 1.0, 1.5, and 2.0*M* KCl. Although it is not possible to interpret rigorously the molecular ellipticities in the wavelength range 200 to 240 nm because of the contributions of both protein and DNA in this region, the lack of systematic change in this region over the range of KCl concentrations (Fig. 2B) is consistent with the conclusion that the α-helix content of the inner histones remains constant when they are in 2*M* NaCl or complexed with DNA.

Raman spectra of ν_1 in 0.2 m*M* EDTA at different temperatures indicated no significant conformational changes in the range 0° to 50°C.

Chicken erythrocyte chromatin in 0.2 m*M* EDTA was a clear gelatinous pellet and exhibited Raman scattering of sufficient quality to reveal its overall similarity to ν_1. Our conclusions regarding the conformations of the histones and DNA in chromatin are therefore the same as for ν_1. One obvious difference is a higher ratio I_{1451}/I_{1489}, consistent with a higher protein/DNA ratio in chromatin, due to the presence of H5 and H1.

The observation that the secondary structure of the inner histones remains the same, whether they are associated with DNA at low ionic strength or devoid of DNA in 2*M* NaCl, is consistent with previous conclusions based on analyses of trypsin digestion products and of the iodination of tyrosine residues of the inner histones (*9*).

Nuclear magnetic resonance studies of the isolated histones have permitted identification of regions in the histone molecules which may be involved in salt-induced self-interactions (*23*). Further, it has been proposed (*23*) that these structured apolar regions are the sites of histone-histone interactions, whereas the basic segments of the histones are the major DNA binding sites. It appears that these basic portions of the histones are not appreciably structured under high-salt conditions, and would therefore not be likely sites for extensive α-helix formation. We suggest that the apolar globular domains of the inner histones are the primary regions of α helix. These structured regions represent approximately 60 percent of the histone sequences. If 50 percent α helix is confined to 60 percent of the histone, these structured regions would approach 80 percent α-helix content, which is comparable to the helix content of myoglobin (*16, 24*). We favor a model for the nu body which consists of a core of closely packed α-helical globular regions of the inner histones (*2*) surrounded by a DNA-rich outer shell. We further suggest that the basic segments of the histones possess little α-helix or β-sheet structure, whether dissociated from or associated with the DNA.

G. J. THOMAS, JR.
B. PRESCOTT
Department of Chemistry, Southeastern Massachusetts University, North Dartmouth 02747
D. E. OLINS
University of Tennessee–Oak Ridge Graduate School of Biomedical Sciences and *Biology Division, Oak Ridge National Laboratory, Oak Ridge 37830*

References and Notes

1. For recent reviews see G. Felsenfeld, *Nature (London)* **257**, 177 (1975); S. C. R. Elgin and H. Weintraub, *Annu. Rev. Biochem.* **44**, 725 (1975); E. M. Bradbury, *Trends Biochem. Sci.* **1**, 7 (1976); P. Newmark, *Nature (London)* **261**, 544 (1976).
2. A. L. Olins, J. P. Breillatt, R. D. Carlson, M. B. Senior, E. B. Wright, D. E. Olins, in *The Molecular Biology of the Mammalian Genetic Apparatus*, part A, P. O. P. T'so, Ed. (Elsevier/North-Holland, Amsterdam, in press); A. L. Olins, R. D. Carlson, E. B. Wright, D. E. Olins, *Nucleic Acid Res.* **3**, 3271 (1976).
3. Nucleic acid applications are reviewed by G. J. Thomas, Jr., in *Vibrational Spectra and Structure*, J. R. Durig, Ed. (Dekker, New York, 1975), vol. 3, pp. 239–315.
4. Protein applications are reviewed by B. G. Frushour and J. L. Koenig, in *Advances in Infrared and Raman Spectroscopy*, R. J. H. Clark and R. E. Hester, Eds. (Heyden, London, 1975).
5. See, for example, G. J. Thomas, Jr., *Appl. Spectrosc.* **30**, 483 (1976) and citations therein.
6. G. J. Thomas, Jr., B. Prescott, P. M. Ordzie, K. A. Hartman, *J. Mol. Biol.* **102**, 103 (1976).

7. G. J. Thomas, Jr., and P. Murphy, *Science* **188**, 1205 (1975).
G. J. Thomas, Jr., and J. R. Barylski, *Appl. Spectrosc.* **24**, 463 (1970).
9. H. Weintraub, K. Palter, F. Van Lente, *Cell* **6**, 85 (1975).
10. Total unfractionated ν_1 consists of DNA fragments of 125 to 180 bp associated with the inner histones and variable amounts of H5 and H1. Dialysis of total ν_1 against 0.1*M* KCl results in a soluble fraction containing equimolar amounts of H4, H3, H2B, and H2A associated with DNA (~ 140 bp), and a precipitated fraction containing all of the histones including H5 and H1 associated with DNA fragments. The products of subfractionation are described in (*2*). Unless stated otherwise, the Raman spectra of ν_1 reported here refer to the KCl-soluble ν_1 fraction (standard sedimentation coefficient at 20°C in water, 11.4; molecular weight, 210,000 to 216,000).
11. B. Prescott, C. H. Chou, G. J. Thomas, Jr., *J. Phys. Chem.* **80**, 1164 (1976).
12. S. E. Erfurth and W. L. Peticolas, *Biopolymers* **14**, 247 (1975); S. Mansy, S. K. Engstrom, W. L. Peticolas, *Biochem. Biophys. Res. Commun.* **68**, 1242 (1976).
13. S. E. Erfurth, E. J. Kiser, W. L. Peticolas, *Proc. Natl. Acad. Sci. U.S.A.* **69**, 938 (1972). To confirm the double helicity of chicken DNA, its Raman spectrum was recorded at several temperatures in the range 0° to 90°C and the hypochromism was measured. The results obtained were similar to those reported for calf thymus DNA (*12*), as long as the chicken DNA solution contained no added salt. However, when either KCl or NaCl was present (salt concentration range, 0.10 to 2.0*M*), the sample exhibited fluorescence of high intensity at temperatures above 70°C and satisfactory Raman spectra could not be recorded. This problem is frequently encountered with biopolymers, especially with deoxyribopolymers. The reagents (KCl and NaCl) themselves exhibited no such fluorescence, and therefore it must be presumed that the salinity is only an indirect causative factor, perhaps "leaching out" a fluorescent contaminant of the DNA or nu body solutions.
M. C. Chen and R. C. Lord, *J. Am. Chem. Soc.* **96**, 4750 (1974).
15. J. L. Lippert, D. Tyminski, P. J. Desmeules, *ibid.* **98**, 7075 (1976).
16. C. C. Baker and I. Isenberg, *Biochemistry* **15**, 629 (1976).
17. Y.-H. Chen, J. T. Yang, K. H. Chau, *ibid.* **13**, 3350 (1974).
18. M. N. Siamwiza *et al.*, *ibid.* **14**, 4870 (1975).
T.-J. Yu, J. L. Lippert, W. L. Peticolas, *Biopolymers* **12**, 2161 (1973).
20. D. E. Olins *et al.*, *Biophys. J.* **17**, 114a (1977); in preparation.
21. J.-E. Germond, M. Bellard, P. Oudet, P. Chambon, *Nucleic Acid Res.* **3**, 3173 (1976).
22. The rather weak Raman lines of the DNA backbone at 1015 and 1143 cm^{-1}, possibly due to C–O and C–C stretching vibrations (*3*), appear to be the only ones affected by the association with inner histones. [It should be mentioned that the results obtained here (Fig. 2) could also be interpreted to mean that ν_1 is not disassociated in 2*M* NaCl at the conditions used for Raman spectroscopy.]
23. E. M. Bradbury and H. W. E. Rattle, *Eur. J. Biochem.* **27**, 270 (1972); E. M. Bradbury *et al.*, *Ann. N.Y. Acad. Sci.* **222**, 266 (1973); see also (*1*). Current assignments of the histone sequences involved in salt-induced self-interactions are: H4, residues 33 to 102, 69 percent of the total sequence; H3, 42 to 110, 51 percent; H2B, 31 to 102, 58 percent; and H2A, 25 to 109, 66 percent. Therefore, the total number of amino acid residues believed to be in the apolar globular domains is 296 of 491 residues, 60 percent of the total inner histone sequence.
24. For an extensive review of the circular dichroic data for histones and chromatin, see G. D. Fasman, P. Y. Chou, and A. J. Adler [in *The Molecular Biology of the Mammalian Genetic Apparatus*, part A, P. O. P. T'so, Ed. (Elsevier/North-Holland, Amsterdam, in press)]. These authors also apply a predictive method to the amino acid sequences of the histones and calculate a maximal α-helix content for the inner histones of 36 percent (averaging their maximal values for the separate histones H4, H3, H2B, and H2A), with 22 percent β-sheet and 43 percent β-turn or random structure. Our results reported here do not support their prediction of considerable β-sheet structure. Whereas Fasman *et al.* incline toward the view that β-sheet–β-sheet interactions between the apolar regions of the inner histones might parallel those in such proteins as insulin and concanavalin A, we suggest that α-helix–α-helix associations between subunits, as in hemoglobin, would better explain our observed high α-helix and negligible β-sheet content in chromatin nu bodies. This view would be consistent with recent estimates of the secondary structure of H3-H4 tetramer (29 percent α helix and no β structure) and the H2A-H2B complex (37 percent α helix and no β structu [T. Moss, P. D. Cary, C. Crane-Robinson, E. M. Bradbury, *Biochemistry* **15**, 2261 (1976); T. Moss, P. D. Cary, B. D. Abercrombie, C. Crane-Robinson, E. M. Bradbury, *Eur. J. Biochem.* **71**, 337 (1976)]. A comparison of these data with our own suggests the possibility that formation of the heterotypic tetramer or the inner histone octamer within ν_1, from the homotypic histone complexes, results in a net increase in α-helix content but no apparent increase in β structure.
25. We thank R. E. Harrington for analyzing the circular dichroic spectra of the inner histones. R. E. Harrington and A. L. Olins critically evaluated the manuscript. E. B. Wright helped in the preparation of materials. This work was supported in part by NIH grants AI 11855 (G.J.T.) and GM 19334 (D.E.O.) and by the Energy Research and Development Administration under contract with Union Carbide Corporation. The results of this investigation were presented at the 21st annual meeting of the Biophysical Society and were published in an abstract [B. Prescott, G. J. Thomas, Jr., D. E. Olins, *Biophys. J.* **17**, 114a (1977)].

14 February 1977; revised 26 April 1977

An Effective Immunization of Experimental Monkeys Against a Human Malaria Parasite, *Plasmodium falciparum*

Abstract. *This is the first report of successful immunization of experimental monkeys against a human malaria parasite,* Plasmodium falciparum. *Of the five owl monkeys* (Aotus trivirgatus) *used in this pilot study, two served as controls and the other three were immunized with* P. falciparum *antigen consisting primarily of mature segmenters containing fully developed merozoites. Two injections of antigen emulsified with Freund's complete adjuvant were administered intramuscularly 3 weeks apart. Three weeks after the second vaccination, all monkeys were challenged with the homologous strain of* P. falciparum. *The control monkeys died with high levels of parasitemia within 2 weeks of challenge. The three immunized monkeys survived and showed strong protection against* P. falciparum. *These results are encouraging for the possible future development of an effective vaccine against human malaria.*

Attempts to develop a vaccine against malaria began half a century ago but gave way to searches for new drugs during World War II and to antimosquito programs afterward. However, resistance to drugs and insecticides and lack of money have reduced the prospects of malaria eradication, and thoughts have again turned to the possibility of developing a malaria vaccine (*1*).

Four different kinds of vaccines are currently under investigation: exoerythrocytic merozoites from tissue culture (*2*), irradiated sporozoites from the mosquito (*3*), extracts from blood schizonts (*4*), and emulsified erythrocytic merozoites (*5*). Most studies of these vaccines were made on bird, rodent, and monkey malarias. This report describes the first successful immunization of owl monkeys (*Aotus trivirgatus*) against infection with a human malaria parasite (*Plasmodium falciparum*).

The Uganda–Palo Alto strain (FUP) of

Table 1. Vaccination of *Aotus* monkeys against *Plasmodium falciparum* [Uganda–Palo Alto strain (FUP)] malaria.

Monkey	Composition of vaccine*					Number of infected erythrocytes in the challenge inoculum¶ (day 44)
	KGS† per injection (ml)	FCA‡ per injection (ml)	Parasite protein (mg) in 0.5 ml KGS (injection 1, day 0)§	Parasite protein (mg) in 0.5 ml KGS (injection 2, day 23)‖	Total parasite protein (mg)	
A266	1.0					6.2×10^5
A267	0.5	0.5				6.2×10^5
A268		0.5	1.83	0.9	2.73	6.2×10^5
A269		0.5	1.83	0.9	2.73	6.2×10^5
A270		0.5	1.83	0.9	2.73	6.2×10^5

*Freund's complete adjuvant plus antigen mixed, using a double-hubbed needle and two syringes. Administered intramuscularly in alternate thighs. †Kreb's glucose saline; No. A266 was given two injections of KGS (intramuscularly) on day 0 and on day 23. ‡Freund's complete adjuvant (Baltimore Biological Laboratory, division of Bioquest); No. A267 was given two injections (intramuscularly) of FCA mixed in KGS on day 0 and on day 23. §More than 60 percent segmenters containing individual merozoites. Remainder of the parasite material consisted of schizonts and mature trophozoites. ‖More than 50 percent segmenters containing individual merozoites. Remainder of the parasite material consisted of schizonts and mature trophozoites. ¶Infected blood was obtained from an ongoing FUP infection. Inoculum was given intravenously.